Published OnlineFirst September 30, 2013; DOI: 10.1158/1078-0432.CCR-12-3580

Clinical Cancer Research

Prostate Cancer Progression Correlates with Increased Humoral Immune Response to a Human Endogenous Retrovirus GAG Protein

Bernardo Sgarbi Reis, Achim A. Jungbluth, Denise Frosina, et al.

Clin Cancer Res 2013;19:6112-6125. Published OnlineFirst September 30, 2013.

Published OnlineFirst September 30, 2013; DOI: 10.1158/1078-0432.CCR-12-3580

Clinical Cancer Research

Prostate Cancer Progression Correlates with Increased Humoral Immune Response to a Human Endogenous Retrovirus GAG Protein

Bernardo Sgarbi Reis[1], Achim A. Jungbluth[1], Denise Frosina[1], Megan Holz[1], Erika Ritter[1], Eiichi Nakayama[8], Toshiaki Ishida[8], Yuichi Obata[9], Brett Carver[2], Howard Scher[3], Peter T. Scardino[2], Susan Slovin[3], Sumit K. Subudhi[3], Victor E. Reuter[4], Caroline Savage[5], James P. Allison[6], Jonathan Melamed[7], Elke Jäger[10], Gerd Ritter[1], Lloyd J. Old[1,†], and Sacha Gnjatic[1]

Abstract

Purpose: Human endogenous retroviruses (HERV) encode 8% of the human genome. While HERVs may play a role in autoimmune and neoplastic disease, no mechanistic association has yet been established. We studied the expression and immunogenicity of a HERV-K GAG protein encoded on chromosome 22q11.23 in relation to the clinical course of prostate cancer.

Experimental Design: *In vitro* expression of GAG-HERV-K was analyzed in panels of normal and malignant tissues, microarrays, and cell lines, and effects of demethylation and androgen stimulation were evaluated. Patient sera were analyzed for seroreactivity to GAG-HERV-K and other self-antigens by ELISA and seromics (protein array profiling).

Results: GAG-HERV-K expression was most frequent in prostate tissues and regulated both by demethylation of the promoter region and by androgen stimulation. Serum screening revealed that antibodies to GAG-HERV-K are found in a subset of patients with prostate cancer (33 of 483, 6.8%) but rarely in male healthy donors (1 of 55, 1.8%). Autoantibodies to GAG-HERV-K occurred more frequently in patients with advanced prostate cancer (29 of 191 in stage III–IV, 21.0%) than in early prostate cancer (4 of 292 in stages I–II, 1.4%). Presence of GAG-HERV-K serum antibody was correlated with worse survival of patients with prostate cancer, with a trend for faster biochemical recurrence in patients with antibodies to GAG-HERV-K.

Conclusions: Preferential expression of GAG-HERV-K ch22q11.23 in prostate cancer tissue and increased frequency of autoantibodies observed in patients with advanced prostate cancer make this protein one of the first *bona fide* retroviral cancer antigens in humans, with potential as a biomarker for progression and biochemical recurrence rate of prostate cancer. *Clin Cancer Res; 19(22); 6112–25. ©2013 AACR.*

Introduction

Human endogenous retroviruses (HERV) are genome modifiers of exogenous origin that became integrated in the human genome millions of years ago and now represent 8% of total DNA sequences. They are classified into 30 to 50 families, family K being the most recently identified (1). HERVs contain genes that encode polyproteins flanked by 2 long terminal repeats (LTR; ref. 2). Most HERV genes have mutations or deletions in their coding and promoter sequence, which compromise their gene and/or protein

Authors' Affiliations: [1]Ludwig Institute for Cancer Research, New York Branch at Memorial Sloan-Kettering Cancer Center; Departments of [2]Surgery, [3]Medicine, [4]Pathology, [5]Biostatistics, and [6]Immunology, Memorial Sloan-Kettering Cancer Center; [7]NYU Langone Medical Center, New York; [8]Department of Immunology, Okayama University Graduate School of Medicine, Dentistry and Pharmaceutical Sciences, Okayama; [9]RIKEN Bioresource Center, Tsukuba, Ibaraki, Japan; and [10]Klinik für Onkologie und Hämatologie, Krankenhaus Nordwest, Frankfurt, Germany

Note: Supplementary data for this article are available at Clinical Cancer Research Online (http://clincancerres.aacrjournals.org/).

Current address for B.S. Reis: Laboratory of Mucosal Immunology, Rockefeller University, 1248 York Avenue, New York, NY 10021; current address for J.P. Allison: Department of Immunology, The University of Texas, MD Anderson Cancer Center, PO Box 1301402, Houston, Texas 77030-1903; current address for G. Ritter: Ludwig Institute for Cancer Research Ltd, New York Office, 666 Third Avenue, New York, NY 10017; and current address for S. Gnjatic: Department of Medicine, Hematology/Oncology, Tisch Cancer Institute, Icahn School of Medicine at Mount Sinai, New York, NY 10021.

†Deceased.

Corresponding Authors: Bernardo Sgarbi Reis, Laboratory of Mucosal Immunology, Rockefeller University, 1248 York Avenue, Smith Hall Building, Room 106, New York, NY 10065. Phone: 212-327-7591; E-mail: breis@mail.rockefeller.edu; and Sacha Gnjatic, Department of Medicine, Division of Hematology/Oncology, Tisch Cancer Institute, Icahn School of Medicine at Mount Sinai, 1470 Madison Avenue, Box 1129, Room 5-105, New York, NY 10029. Phone: 212-824-8438; Fax: 646-537-9577; E-mail: sacha.gnjatic@mssm.edu

doi: 10.1158/1078-0432.CCR-12-3580

Published OnlineFirst September 30, 2013; DOI: 10.1158/1078-0432.CCR-12-3580

Translational Relevance

Prediction of prostate cancer progression and mortality has relied on several known biomarkers, including Gleason score, serum prostate-specific antigen (PSA), and prostate specific membrane antigen (PSMA) levels. Here, we explore the expression and immunogenicity of a new endogenous retroviral antigen that correlates with progression of prostate cancer. This antigen was found in primary and metastatic prostate cancer tissues and cell lines, and we described mechanisms driving its specific expression. Moreover, the spontaneous serum antibody response to this antigen in a large number of patients with prostate cancer revealed an association with clinical progression of cancer. As a result, we propose that measuring expression and serological responses for this new antigen could have a rapid impact on the clinical course and management of prostate cancer. In a long-term perspective, modulating the immunogenicity to a retroviral endogenous antigen would be a novel immunointervention strategy.

expression. In addition, HERV expression in normal tissue is usually suppressed by DNA methylation (3–6).

Endogenous retroviruses have been closely linked as the etiologic agent to a wide variety of animal cancers. One of the best examples is the MuLV, a mouse endogenous retrovirus associated with leukemia in murine hosts (7, 8). Serologic techniques have been critical in establishing the complex relation between these viruses and their hosts (9–12). Our group developed a powerful approach for detecting cancer antigens based on patient humoral immune response (13, 14). Taking advantage of this technique and by using a prostate cancer serum sample, we previously identified a GAG protein derived from human endogenous retrovirus K located on chromosome 22q11.23 (*GAG-HERV-K ch22q11.23, NGO-Pr-54*; ref. 15). This endogenous retrovirus has been associated with chromosomal rearrangements occurring in prostate cancer that create fusion genes in which the promoter region of *GAG-HERV-K ch22q11.23* translocates downstream of *ETV1* gene leading to abnormal expression of ETS transcriptional factor (16, 17).

Despite the fact that most HERVs have mutated or deleted coding sequences, intact open reading frames (ORF) exist and give rise to transcripts that can be detected by real-time PCR (qPCR; refs. 15, 18, 19). Although no expression at the protein level has been clearly identified, immune responses against various HERV components have been widely shown in different types of cancer, including prostate cancer (20–24). However, a clear correlation between immune response to HERV components and clinical stage has not been intently addressed in prostate cancer.

Prostate cancer is one of the most frequent causes of male cancer-related deaths (25). Clinical staging of prostate cancer is important in assessing the risk of the disease and therefore for treatment recommendations (26). Still, improved clinical staging biomarkers are required for more reliable prediction of pathologic stage in prostate cancer (27–30). The discovery of an endogenous retrovirus antigen highly expressed in prostate cancer and able to elicit humoral immune responses related to disease progression makes this an attractive potential new biomarker for clinical staging and a novel target for immunotherapy. In this work, we explore the correlation between humoral immune response to HERV antigen and cancer progression and show mechanisms that could be contributing to HERV activity in prostate cancer.

Materials and Methods

Patient samples and cell lines

Sera were collected with informed consent under protocols approved by the Institutional Review Board of Memorial Sloan-Kettering Cancer Center (New York, NY) and by the Ethics Review Board from Krankenhaus Nordwest (Frankfurt, Germany). Serum samples were collected at Memorial Sloan-Kettering Cancer Center or provided by Dr. Elke Jäger from Krankenhaus Nordwest, typically at time of diagnosis. Prostate cancer patient sera were divided according to clinical stage of the disease (I–IV) using the TNM classification system (American Joint Committee on Cancer), as well as according to Gleason score whenever available. Patient characteristics for a subset of patients are shown in Table 1. Cell lines were derived at Memorial Sloan-Kettering Cancer Center or purchased from American Type Culture Collection. All human cell lines were maintained in RPMI containing 10% FBS, 1% L-glutamine at 37°C in a 5% CO_2 atmosphere.

Probes and monoclonal antibodies

The IgG1 monoclonal antibody to anti-GAG-HERV-K, clone TI-35, was previously generated by our group (15). Antibodies for human androgen receptor (AR-441 - clone ab9474, 1:1,000) and actin (clone ab8227, 1:10,000) were obtained from Abcam. TaqMan primers and probes for *KLK3* (PSA), *BCR*, *ZDHHC8P1*, *IGGL1*, *RGL4*, and *TFRC* genes were obtained from Amersham Bioscience. *GAG-HERV-K* primers sequences were GAG22q11.23-F (5′-CGC AGG TTA GAC AAG CAC AA-3′) and GAG22q11.23-R (5′-CTC AAG ATC GCC CTG TTT TC-3′).

RNA extraction

RNA extraction was conducted using TRIzol Reagent (Gibco), according to manufacturer's instructions with few modifications. Briefly, 5×10^6 to 10×10^6 cells or 100 mg of cancer tissue were homogenized with 1 mL TRIzol reagent and incubated for 5 minutes at room temperature. Two drops of OCT and 100 μL BCP were added to the solution and vortexed. The samples were centrifuged for 15 minutes at 4°C, and the aqueous phase was collected for RNA precipitation by isopropanol. The resuspended RNA was submitted to DNase treatment according to manufacturer's instructions (Ambion). The concentration was determined using NanoPhotometer (IMPLEM). Total RNA derived from normal tissues was obtained from Clontech and Ambion.

Published OnlineFirst September 30, 2013; DOI: 10.1158/1078-0432.CCR-12-3580

Table 1. Patient characteristics within group analyzed by Kaplan–Meier

	Localized, low risk[a] $n = 102$	Localized, high risk[a] $n = 96$	Metastases[a] $n = 86$
Age at biopsy	59 (54–64)	62 (56–65)	61 (56–65)
PSA	6.42 (4.10–8.80)	9.40 (5.20–16.00)	9.50 (6.10–17.80)
Pathologic Gleason grade			
≤6	102 (100%)	1 (1%)	3 (6%)
7	0 (0%)	14 (20%)	20 (42%)
≥8	0 (0%)	56 (79%)	25 (52%)
Pathologic stage > T2	8 (8%)	78 (82%)	50 (59%)
Positive surgical margins	11 (11%)	34 (36%)	40 (47%)
Extracapsular extension	0 (0%)	69 (73%)	42 (49%)
Seminal vesicle invasion	0 (0%)	40 (42%)	33 (39%)
Lymph node involvement	0 (0%)	15 (16%)	21 (26%)
Neoadjuvant	16 (16%)	49 (51%)	42 (49%)
Adjuvant	0 (0%)	7 (7%)	8 (9%)
Type of surgery			
Open	102 (100%)	83 (86%)	80 (94%)
Laparoscopic	0 (0%)	2 (2%)	0 (0%)
Salvage	0 (0%)	11 (11%)	5 (6%)
Received radiation	1 (1%)	22 (23%)	14 (16%)

NOTE: Age and PSA values are median (interquartile range).
[a]Samples obtained at time of surgery or biopsy and assessed retrospectively.

Real-time PCR

cDNA was generated from 2 μg of total RNA using the SuperScript First Strand Synthesis System for RT-PCR (Invitrogen), according to manufacturer's instructions. Real-time PCR was carried out using Sybr-green Master Mix (Invitrogen) for *GAG-HERV-K chr22q11.23* or TaqMan Master Mix (ABI) for *AR* and *KLK3* (PSA) on an ABI Prism 7500 Fast real-time PCR system machine (Applied Biosystems) using specific primers and probes. Relative PCR analysis was completed using ABI Prism SDS software. Real-time PCR products were analyzed by electrophoresis and by sequencing. *GAPDH* (Sybr-green system) and *TFRC* (TaqMan system) were used as housekeeping genes.

TI-35 mAb characterization

The generation and characterization of mAb TI-35 was previously described by our group (15). In addition, transfection of HeLa cells with *GFP*-fused *GAG-HERV-K* construct or control *GFP* was conducted to assess the subcellular localization of TI-35 staining by confocal microscopy and immunofluorescence. TI-35 specificity was further assessed by immunohistochemistry (IHC) with formalin-fixed, snap-frozen pellets of Sf9 insect cells infected with *GAG-HERV-K* recombinant or control baculovirus. In addition, TI-35 reactivity was assessed by Western blotting and ELISA against GAG-HERV-K synthetic overlapping long peptides, recombinant GAG-HERV-K proteins produced in *Escherichia coli* and baculovirus as well as control proteins, and cell extracts from GAG-HERV-K–positive VCaP cells before and after treatment with androgen (see details below).

Immunohistochemistry

For the immunohistochemical detection of GAG-HERV-K, monoclonal antibody TI-35 was used. TI-35 immunostaining was done in snap-frozen specimens as well as in formalin-fixed, paraffin-embedded tissue. For paraffin sections, 0.5 μg/mL of TI-35 using EDTA (pH 9.0, 1 mmol/L) as antigen retrieval solution achieved best staining results. For primary detection, the Powervision Kit (Leica Biosystems) was used. Immunohistochemical staining was done on 5-μm tissue sections applied to slides for IHC (Superfrost Plus, Menzel). Slides were heated for proper attachment at 60°C for 3 hours. For immunostaining, slides were deparaffinized in xylene and rehydrated in a series of graded alcohols followed by antigen retrieval. The latter consisted of heating slides in EDTA solution at 97°C for 30 minutes. Primary incubation was done overnight at 4°C followed by the powervision secondary. Diaminobenzidine (liquid-DAB, Biogenex) served as a chromogen, and Gill's #2 hematoxylin was used as a counterstain.

Because mAb TI-35 stained many tissues with different intensity, intensity of staining was scored in addition to the more classic extent of staining. The immunoreactivity of TI-35 was graded on the basis of extent of immunopositive tumor areas as follows: negative (0), focal, that is, <5% (1), 5%–25% (2), 25%–50% (3), 50%–75% (4), and >75% (5) of TI-35–positive tumor cells. Intensity of staining was graded as weak (1), moderate (2), and intense (3). On the basis of our experience with other mAb to cancer antigens, there was more weight given to the extent of staining (on a scale of 0–5) than to intensity of staining (1–3). Cases with

Published OnlineFirst September 30, 2013; DOI: 10.1158/1078-0432.CCR-12-3580

moderate (2) and intense (3) staining in more than 50% of the tumor (4 and 5) were considered "strong" expressers; "moderate/weak" expressers were cases with weak (1) staining irrespective of extent and cases with staining in less than 50% of the tumor (1–3) irrespective of intensity.

Induction of *GAG-HERV-K ch22q11.23* expression by 4,5α-dihydrotestosterone

Cancer cell lines were submitted to 4,5α-dihydrotestosterone (DHT; Sigma-Aldrich) stimulation as described before (31). Briefly, 2×10^5 cells were cultured in a 35-mm culture dish for 48 hours in RPMI 10% fetal calf serum (FCS) media at 37°C. The cells were then treated with 0.1, 1, or 10 nmol/L of DHT for another 48 hours. Cells were then harvested for RNA extraction and qPCR evaluation of *GAG-HERV-K* expression, as described previously. The results were expressed as fold increase relative to untreated cells. Cells were also harvested for protein extraction and Western blot analysis.

Luciferase assay

Cancer cell lines VCaP were plated at 5×10^4 cells per well in a 96-well plate in RPMI 10% FCS medium at 37°C. Twenty-four hours later, cells were transfected with pGL3-promoter plasmid (Promega) carrying the 5′LTR promoter region of *GAG-HERV-K*. Cells were incubated for an extra 8 hours and then treated for 48 hours with or without 1 nmol/L DHT. The empty pGL3-promoter plasmid was used as control (mock). Cells were harvested and assayed for luminescence count according to manufacturer's protocol (Promega).

Methylation status of the *HERV-K ch22q11.23* promoter region (5′LTR)

The gDNA from cancer cell lines was extracted using DNeasy kit (Qiagen) according to manufacturer's instructions. The methylation status was evaluated by adapting the Methyl-Profiler DNA Methylation PCR Array System protocol (SA Bioscience). Briefly, gDNA from cancer cell lines was incubated with methylation-sensitive restriction enzyme (Ms), methylation-dependent restriction enzyme (Md), both (Msd) or any (Mo) and the promoter region was amplified by real-time PCR using specific primers (methyl-F 5′-ATG TGC CTT GTT AAC AAT GTG TTT A-3′ and methyl-R 5′-CTC AAC TGC AAG AGG CCT TC-3′). The methylation status was calculated by the following formula: PMS = 1 − F_{UM}, where PMS = promoter methylation status; F_{UM} (unmethylated fraction) = $2^{\wedge}-(C_{t\_Md} - C_{t\_Mo})$. The enzyme digestion efficiency (W) was calculated as $W = 100 - [100 \times (2^{\wedge}-(C_{t\_Mo} - C_{t\_Msd}))]$. Seventy per cent cutoff digestion efficiency was adopted for experiment validation.

Induction of *GAG-HERV-K ch22q11.23* expression by 5-aza-2′-deoxycitidine treatment

The influence of DNA demethylation in *GAG-HERV-K* expression was evaluated by 5-aza-2′-deoxycitidine treatment. Briefly, 2×10^5 cells were cultured in a 35-mm culture dish for 48 hours in RPMI 10% FCS medium at 37°C. The cells were then treated with 0.1 or 1 mmol/L of 5-aza-2′-deoxycitidine for another 48 hours. Cells were then washed with PBS and cultured for another 48 hours at 37°C in RPMI 10% FCS in the presence or absence of DHT. Cells were then harvested for RNA extraction and qPCR evaluation of *GAG-HERV-K* expression, as described previously. The results were expressed as fold increase relative to untreated cells.

SDS-PAGE and Western blot

Cell lines were cultured in RPMI 10% FCS and subjected to protein extraction using modified radioimmunoprecipitation assay (RIPA) buffer. The protein extract was submitted to continuous electrophoresis using NuPAGE 4%–12% Bis–Tris gel (Invitrogen), under reducing conditions. The separated proteins were transferred to polyvinylidene difluoride (PVDF) membrane and incubated with blocking solution [3% bovine serum albumin (BSA), 0.15 mol/L PBS, pH 7.4] for 1 hour at room temperature and then incubated with human sera diluted 1:10,000 or TI-35 mouse monoclonal antibody diluted 1:1,000 in dilution buffer (1% BSA, 0.15 mol/L PBS, pH 7.4) for 16 hours at 4°C. The membranes were then washed (0.2% Tween-20, 0.15 mol/L PBS, pH 7.4) and incubated with goat anti-human IgG peroxidase-conjugated diluted 1:1,000 (Southern Biotech) or rabbit anti-mouse peroxidase-conjugated (Sigma) diluted 1:20,000 in dilution buffer, for 1 hour at room temperature. Membranes were developed with Western Lighting Plus-ECL solution (Perkin Elmer Inc).

ELISA

ELISA assays were conducted as previously described (32). Briefly, plasma was serially diluted from 1:100 to 1:2,500, added to low-volume 96-well plates (Corning) coated with 0.25 μg/mL full-length recombinant GAG-HERV-K protein or negative control protein DHFR, or with 1 μmol/L GAG-HERV-K overlapping 20mer peptides, and blocked with PBS containing 5% non-fat milk. After incubation, plates were washed by automatic plate washer (Bio-Tek) with PBS containing 0.2% Tween and rinsed with PBS. Total IgG bound to antigens was detected with alkaline phosphatase–conjugated anti-human IgG monoclonal antibody (Southern Biotech). Following addition of ATTOPHOS substrate (Fisher Scientific), absorbance was measured. A reciprocal titer was extrapolated by determining the intersection of a linear trend regression with a cutoff value. The cutoff was defined as 7.5× the average of the OD values from the 3 dilutions of a negative control pool of 4 healthy donor sera. Sera with reciprocal titers >100 to GAG-HERV-K but without reactivity to DHFR were considered significant after confirmation in repeat titration assays.

GAG-HERV-K_GFP fusion protein expression in HeLa cells and baculovirus

GAG-HERV-K gene was amplified using specific primers (pIC113-F 5′-AACTCGAGATGGGGCAAACTGAAAGTAAA-T-3′ and pIC113-R 5′-AAAAGCTTCTACTGCGGTGCTG-CCTG-3′). The amplified product was digested with *Xho*I

Published OnlineFirst September 30, 2013; DOI: 10.1158/1078-0432.CCR-12-3580

and *Hin*dIII restriction enzymes and cloned into plasmid pIC113 containing *GFP* and G418 resistance genes (33). The plasmid was then transfected into HeLa cells using Effectene reagent (Qiagen) and 48 hours after the cells were split 1:10 in a 30-cm^2 plate with RPMI 10% FCS media containing 500 μg/mL G418 selection reagent (Gibco). Two days after selection, positive transfected cells were fixed with 4% formaldehyde and permeabilized with 10% Triton-X. Cells were then stained with TI-35 antibody and analyzed by confocal microscopy (LSM710 Zeiss). Recombinant baculovirus preparation using *GAG-HERV-K* plasmid or control was conducted following manufacturer's instructions (Invitrogen) and used to infect Sf9 insect cells (MOI = 1).

Protein microarray

Arrays were custom-made from version 4 ProtoArrays by Invitrogen with the addition of GAG-HERV-K recombinant protein and used per manufacturer's instructions. For antibody hybridization, arrays were blocked for 1 hour and incubated for 90 minutes at 4°C with individual sera diluted 1:500 in 4 mL buffer [1 mol/L HEPES, pH 7.5, 5 mol/L NaCl, 0.1% Triton X100 (v/v), 25% glycerol (v/v), 20 mmol/L reduced glutathione, 1 μmol/L dithiothreitol (DTT) 10% Synthetic Block solution (Invitrogen) in H_2O] in dishes placed on a horizontal shaker (50 rpm). After 3 washes [0.1% Tween 20 (v/v), 10% Synthetic Block solution (Invitrogen) in PBS], total bound IgG was detected by incubation with Alexa-Fluor 647 goat anti-human IgG (Invitrogen) diluted 1:2,000 in assay buffer for 90 minutes at 4°C. Arrays were washed again and dried by centrifugation. The slides were scanned at 10 μm resolution using a microarray scanner (Axon 4200AL with GenePix Pro Software, Molecular Devices) and fluorescence detected according to the manufacturer's instructions. Images were saved as 16-bit tif files, and analysis was conducted using GenePix. Local backgrounds were subtracted automatically, and the median net intensity in relative fluorescence units (rfu) was reported for each spot. The results were calculated as previously described (34).

Statistical analyses

Statistical analyses for comparing multiple columns were done by one-way ANOVA and with unpaired *t* test for 2-column comparisons. Frequency of patients with seropositive versus seronegative responses was compared using 2-tailed Fisher exact test. Analyses of overall survival and recurrence rates were conducted using the Kaplan–Meier method and analyzed by log-rank or by Gehan–Breslow–Wilcoxon.

Results

Expression of GAG-HERV-K ch22q11.23 in cancer cell line and cancer tissues

We evaluated the expression pattern of *GAG-HERV-K ch22q11.23* in normal and cancer tissues as well as in cancer cell lines by qPCR. As this gene has no introns, RNA was pretreated with DNase to remove gDNA before reverse transcription. The expression of *GAG-HERV-K* was highly restricted in normal tissue, with low levels in prostate, breast, and thyroid (Fig. 1A). *GAG-HERV-K* expression analysis in a large number of tumor cell lines showed absence of detectable expression in most lines from various cancer types. However, significant expression of *GAG-HERV-K* could be detected in some prostate cancer cell lines (VCaP, 22RV-1) and teratocarcinoma cell line (Tera-1; Fig. 1B). Real-time qPCR analysis of *GAG-HERV-K ch22q11.23* expression in prostate cancer tissue showed high expression in 11 of 11 samples. We found that expression of *GAG-HERV-K* was mostly restricted to prostate cancer and generally not present in various other cancer tissue samples such as melanoma, breast cancer, colon cancer, renal cancer, ovarian cancer, esophageal cancer, bladder cancer (except one), lung cancer, and hepatocarcinoma (Fig. 1C and Supplementary Fig. S2). We also evaluated neighboring genes located on chromosome 22q11.23 to check for unspecific transcription of *GAG-HERV-K* in prostate cancer samples due to chromatin remodeling that would favor local gene expression (Supplementary Figs. S1 and S2; ref. 35). Neighboring gene *BCR* was widely expressed in all cancer samples, whereas *IGLL1* and *RGL4* were not significantly altered in any of the cancer samples analyzed. The only gene that displayed a specific increase in prostate cancer was *ZDHHC8P1* (Supplementary Fig. S2). This analysis implies that expression of *GAG-HERV-K ch22q11.23* is specific to prostate cancer. Although we detected high expression of *GAG-HERV-K* in all primary prostate cancer tissues analyzed (Fig. 1C), only 2 of 6 prostate cancer–derived cell lines were positive (Fig. 1B). The difference in *GAG-HERV-K* expression observed between prostate cancer cell lines and prostate cancer tissues may be explained by loss of environmental stimuli after *in vitro* culture such as steroid hormones.

Stimulation of GAG-HERV-K ch22q11.23 expression by DHT *in vitro*

To address the importance of steroid hormones on *GAG-HERV-K* expression, androgen receptor (AR)-positive cell lines (VCaP and LNCaP) and AR-negative cell line (PC-3) were stimulated using different concentrations of DHT. As a positive control for DHT treatment, the expression of *KLK3* (PSA) gene was evaluated before and after DHT stimulation. Expression of GAG-HERV-K was evaluated by qPCR and Western blotting (Fig. 2A). *GAG* sequences from different HERV-Ks are highly homologous. To specifically detect GAG-HERV-K from ch22q11.23, we took advantage of a monoclonal antibody TI-35 previously described by our group (15). This antibody is capable of recognizing an epitope of GAG-HERV-K that contains several nonconserved amino acids (Supplementary Fig. S3A and S3C). Furthermore, TI-35 monoclonal antibody staining colocalized with GFP in HeLa cells expressing GAG-HERV-K_GFP fusion protein (Supplementary Fig. S4A and S4B) showing its high specificity to the GAG-HERV-K antigen. GAG-HERV-K–specific staining of TI-35 was also confirmed in insect cells expressing baculovirus-encoded *GAG-HERV-K*

Published OnlineFirst September 30, 2013; DOI: 10.1158/1078-0432.CCR-12-3580

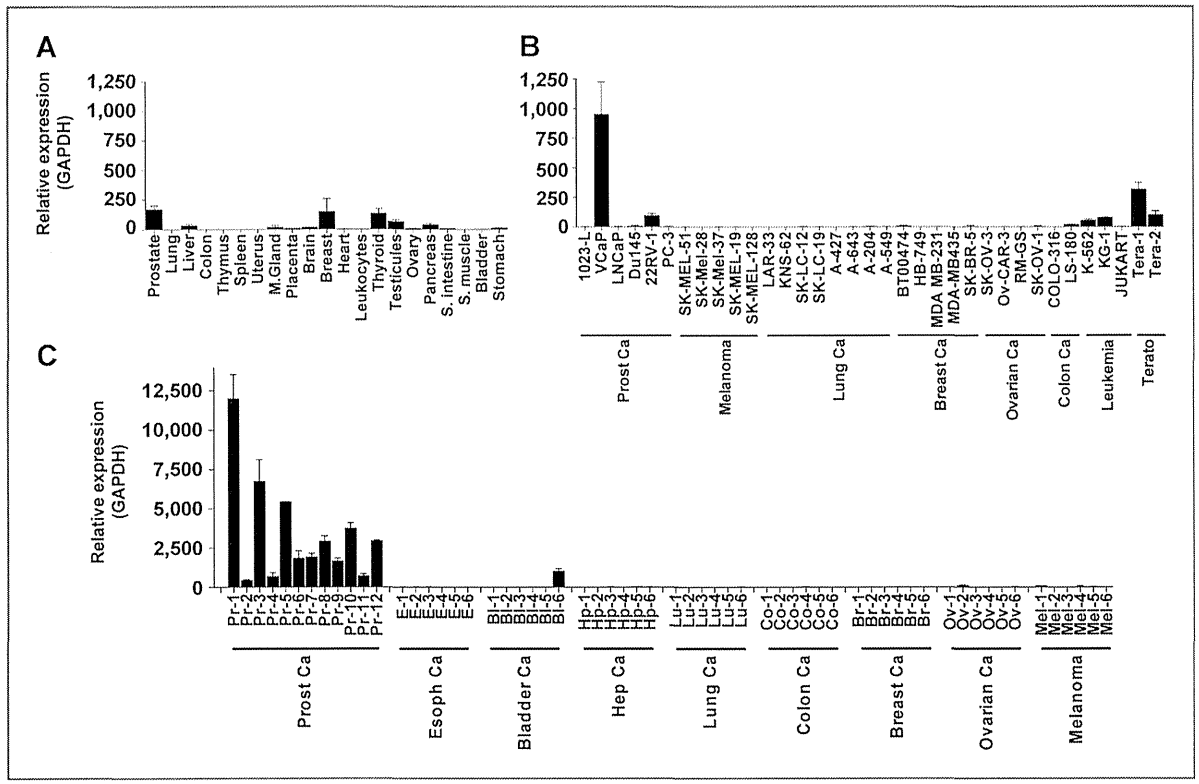

Figure 1. Real-time qPCR expression analysis of *GAG-HERV-K* in normal tissues, cancer cell lines, and cancer tissues. Total RNA from normal tissues, cancer cell lines, or cancer tissues was submitted to DNase treatment and reverse transcriptase reaction for cDNA synthesis. The resulting cDNA was used on qPCR reactions to detect the expression of *GAG-HERV-K ch22q11.23*. The results are expressed as relative expression to housekeeping gene *GAPDH*. A–C, expression of *GAG-HERV-K ch22q11.23* in a normal tissue panel (A), cancer cell lines (B), and in cancer tissues samples (C). Ca, cancer; Prost, prostate; Esoph, esophageal; Hep, Hepatocellular.

or control, using chromogen-based IHC, immunofluorescence, and Western blotting (Supplementary Fig. S4C and S4D and not shown).

DHT treatment was able to increase the expression of GAG-HERV-K in VCaP cell line, both at RNA and protein levels, but not in any other cell line tested (Fig. 2A). Although LNCaP express *AR* (Fig. 2B, left), DHT is not sufficient to induce *GAG-HERV-K* expression in this cell line (Fig. 2A). PC-3 cells do not express AR and, as expected, did not respond to DHT stimulation. *KLK3* (PSA) expression in both LNCaP and VCaP was increased after DHT stimulation (Fig. 2B, right). Increased expression of GAG-HERV-K in VCaP cells was confirmed by immunohistochemical analysis of VCaP cells with mAb TI-35. While unstimulated VCaP cells showed only weak and focal immunostaining with mAb TI-35, VCaP cells stimulated with 10 or 100 nmol/L of DHT exhibited a more intense immunostaining (Fig. 2C).

To evaluate the direct effect of AR in *GAG-HERV-K* expression, the promoter region (5′LTR) of HERV-K was cloned into a luciferase reporter plasmid and transfected into VCaP cells. Cells transfected with the promoter construct or the empty plasmid were cultured in the presence or absence of 10 nmol/L DHT. Luciferase signal could be detected only in cells carrying the HERV-K promoter construct, and DHT stimulation increased the signal compared with unstimulated cells (Fig. 2D). These results suggest that DHT plays an essential role in regulating the expression levels of GAG-HERV-K ch22q11.23 in prostate cancer cell lines.

Role of methylation of the *HERV-K chr22q11.23* promoter region in prostate cancer cell lines

In addition to the role of androgens on GAG-HERV-K expression, we explored the role of DNA methylation, a known mechanism for suppressing HERV expression (3–5, 36). A recent article showed that *HERV-K ch22q11.23* is preferentially expressed in hypomethylated prostate cancer cell lines and primary prostate tissue samples (37). We confirmed these observations by showing that the HERV-K promoter region (5′LTR) of *GAG-HERV-K* negative cell lines (LNCaP and PC-3) was hypermethylated when compared with positive cell line VCaP (Fig. 3A), in accordance with *GAG-HERV-K* expression levels in these lines (Fig. 1B). Moreover, VCaP cells that were simultaneously treated with 5-aza-2′dC and stimulated with 1 nmol/L of DHT showed increased expression of *GAG-HERV-K* compared with cells that were solely DHT-stimulated. This effect was

Published OnlineFirst September 30, 2013; DOI: 10.1158/1078-0432.CCR-12-3580

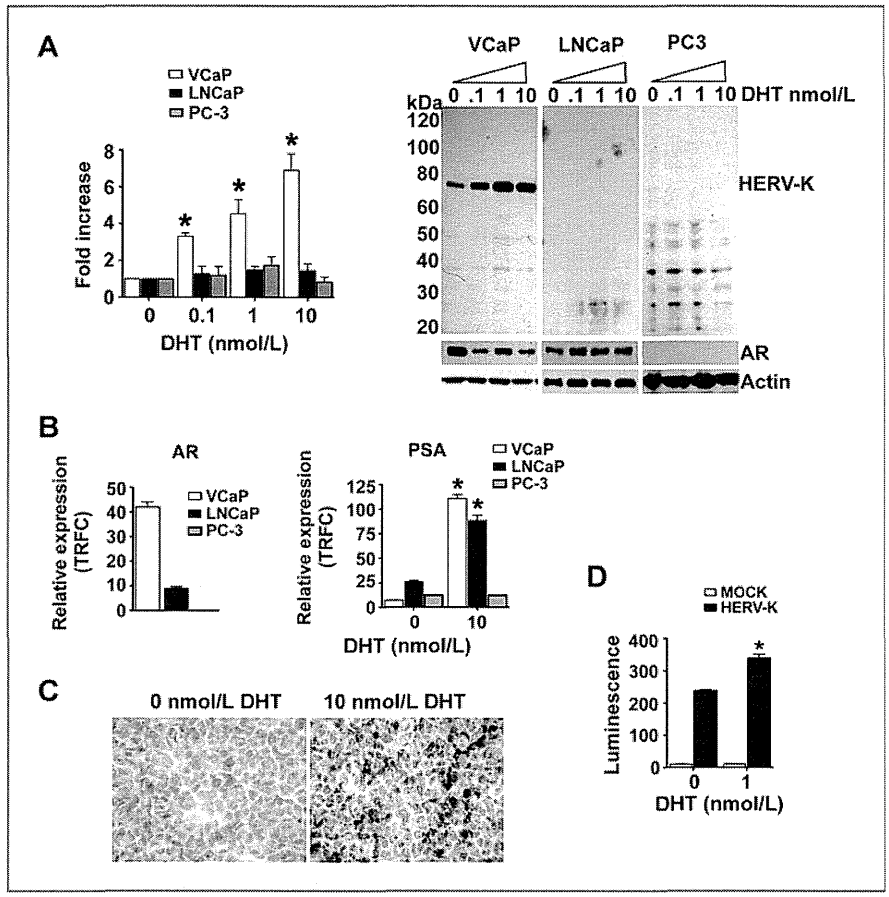

Figure 2. Regulation of GAG-HERV-K expression by DHT in prostate cancer cell lines. A, prostate cancer cell lines were treated with different concentrations of DHT and GAG-HERV-K expression was evaluated by qPCR (left) and Western blotting (right). In qPCR, HERV-K expression levels were relative to housekeeping *GAPDH* and plotted as fold increase compared with untreated cells. In the Western blot analysis, membrane were stained with monoclonal antibody TI-35 (HERV-K), anti-AR, or anti-actin (actin) antibodies. B, qPCR analysis of *AR* expression level in prostate cancer cell lines at steady state (left) and *KLK3* (PSA) expression level before and after treatment with 10 nmol/L of DHT (right). C, immunohistochemical analysis of GAG-HERV-K expression in paraffin sections of VCaP cell pellets showing low-level expression in pellets of native VCaP cells (left) and increased expression after DHT stimulation (right). D, luciferase assay on VCaP cells transfected with pGL3 luciferase reporter plasmid carrying the HERV-K promoter region (HERV-K) or not (MOCK). Cells were incubated with or without 1 nmol/L DHT for 48 hours and harvested for luminescence count. AR and PSA gene expression levels relative to housekeeping gene TRFC using TaqMan probes. *, $P < 0.05$ as indicated compared with data with no DHT.

independent of 5-aza-2′dC concentrations (Fig. 3B, top). LNCaP and PC-3 cell lines did not show increase in *GAG-HERV-K* expression after androgen stimulation (Fig. 3B, middle and bottom). However, 5-aza-2′dC treatment alone was sufficient to induce expression of *GAG-HERV-K* in all tested cell lines (Fig. 3C). Taken together, these results suggest that DNA demethylation together with steroid responsiveness act together to induce *GAG-HERV-K ch22q11.23* expression in prostate cancer cell lines.

Expression of GAG-HERV-K protein in prostate cancer and normal tissues

After optimization of the immunostaining, a panel of normal tissues was analyzed for GAG-HERV-K protein expression using mAb TI-35. Normal skin, lung, liver, and colon were all negative for staining, with the exception of alveolar macrophages. In kidney tissue, there was granular reactivity in epithelia of the proximal and partially distal tubuli as well as in acini of the pancreas (data not shown). We assessed expression of GAG-HERV-K in prostate using a tissue microarray (TMA) with specimens from primary cancer tissue, benign prostate hyperplasia, and normal prostatic tissue, collected at surgery (Fig. 4A and B). Of the 204 cancer cases of the TMA block, 188 cases were evaluable for IHC. According to our grading system, 93 of 188 (49.5%) cases showed strong immunoreactivity (Fig. 4A, bottom), whereas 66 of 188 (35.1%) displayed moderate-to-weak staining with mAb TI-35 (Fig. 4A, middle); 29 of 188 (15.4%) cases remained completely negative (Fig. 4A, top). The association between strong immunoreactivity to GAG-HERV-K and prostate cancer was significant regardless of whether intermediate/weak cases were considered

Published OnlineFirst September 30, 2013; DOI: 10.1158/1078-0432.CCR-12-3580

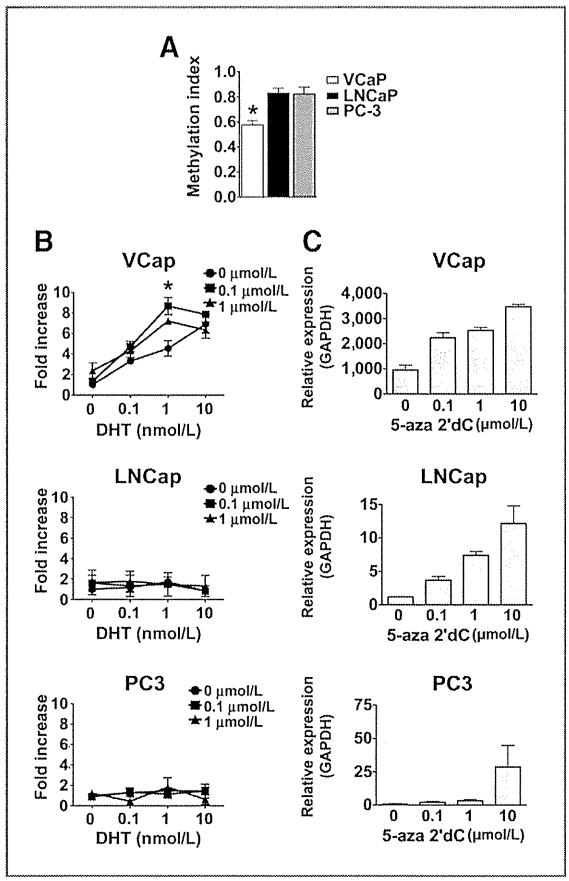

Figure 3. Regulation of *GAG-HERV-K* expression in prostate cancer cell lines. A, HERV-K promoter methylation status on prostate cancer cell lines was determined by methyl-dependent or sensitive enzymatic gDNA digestion and the promoter region was amplified by qPCR. 1 = 100% methylated. B, prostate cancer cell lines were treated with different concentrations of 5-aza-2′dC) and then stimulated with DHT. *GAG-HERV-K* expression was evaluated by qPCR and plotted as fold increase from untreated cells. VCaP cells (top), LNCaP cells (middle), and PC-3 cells (bottom) were evaluated. ● 0 μmol/L of 5-aza-2′dC; ■ 0.1 μmol/L of 5-aza-2′dC; ▲ 1 μmol/L of 5-aza-2′dC. *, $P < 0.05$ compared with other lines (A) or to no 5-aza-2′dC (B). C, prostate cancer cell lines were treated with different concentrations of 5-aza-2′dC. *GAG-HERV-K* expression was evaluated by qPCR and plotted as relative expression to housekeeping gene *GAPDH*. (Top) VCaP cells, (middle) LNCaP cells, and (bottom) PC-3 cells were evaluated. *, $P < 0.05$.

negative or positive. In addition to prostate cancer, the TMA contained 22 samples of normal prostate, 13 of which (59%) were negative and the remaining 9 (41%) displayed weak GAG-HERV-K expression (Fig. 4D). Finally, we analyzed whole block sections of 12 metastatic sites of prostate cancer. All the metastases cases were positive, with 9 of 12 showing strong and 3 of 12 weak expression (examples in Fig. 4C).

To assess protein distribution within other tumor types than prostate, we analyzed whole sections of a limited number of other malignant tumors by IHC with mAb TI-35. We did not see staining with TI-35 in 2 of 2 colon cancers; similarly, 7 of 7 SQCC of the head and neck were completely negative (not shown). However, some tumor types showed staining with TI-35: 1 of 3 melanomas was positive; 1 of 4 non–small cell lung carcinoma (NSCLC) was positive; 2 of 6 breast carcinomas (invasive ductal type, Fig. 4C, bottom) were positive; and 3 of 3 ovarian carcinomas were positive. This indicates that GAG-HERV-K protein expression may not be limited to prostate cancer.

Antibodies against GAG-HERV-K ch22q11.23 in cancer patient sera

Humoral immune responses against HERV proteins have been identified in different cancer types (15, 23, 24). To evaluate immune responses against GAG-HERV-K ch22q11.23 protein in patients with cancer, sera from individual patients with different cancer types ($N = 1367$), as well as healthy donors ($N = 148$), were screened by ELISA for the presence of specific antibodies to recombinant GAG-HERV-K protein. Reciprocal titers were extrapolated from titration curves and results were considered significant if a serum significantly reacted at dilutions greater than the cutoff of 100. We found that 6.8% (33 of 483) of patients with prostate cancer (all stages combined) had serum antibodies to the GAG-HERV-K protein, with a mean reciprocal titer of 2400 (Fig. 4D, left). Interestingly, despite no detectable *GAG-HERV-K* expression among tumor lines analyzed in our panel by qPCR, patients with melanoma (15 of 226; 6.6%), patients with breast cancer (7 of 101; 6.9%), and patients with ovarian cancer (6 of 98; 6.1%) showed similar frequencies of serum antibodies against GAG-HERV-K, albeit with much lower mean titers (<125) than those observed in the prostate cancer group (mean = 2,400; Fig. 4D, left). While commonly observed in prostate cancer, very high titers (>1,000) were elicited in only a few patients with melanoma or ovarian cancer, even though these tumor types also show some GAG-HERV-K tissue expression at the protein level by IHC. All other cancer types analyzed showed less than 5% of patients with anti-GAG-HERV-K autoantibodies, with very weak titers. A similar result was observed in the healthy donor group where 4 individuals (4 of 148; 2.7%) had serum antibodies capable of reacting to the GAG-HERV-K protein with titers above 100 (Fig. 4D, left). These results suggested once more the importance of GAG-HERV-K expression in prostate cancer. To further evaluate the specificity of spontaneous serum autoantibodies to GAG-HERV-K, we used patient sera to immunoprecipitate (IP) naturally expressed GAG-HERV-K protein from VCaP cells. High titer serum from a prostate cancer patient seropositive for anti-GAG-HERV-K was successful in recovering the GAG-HERV-K protein from VCaP cells (Supplementary Fig. S3B). We also mapped the recognition of individual epitopes from GAG-HERV-K using overlapping peptides spanning the entire amino acid sequence. We found that most patient sera reacted to the N-terminal area 101–290 of the antigen or to the C-terminal area 661–690 (Supplementary Fig. S3C). We decided to further investigate the correlation between prostate cancer

Published OnlineFirst September 30, 2013; DOI: 10.1158/1078-0432.CCR-12-3580

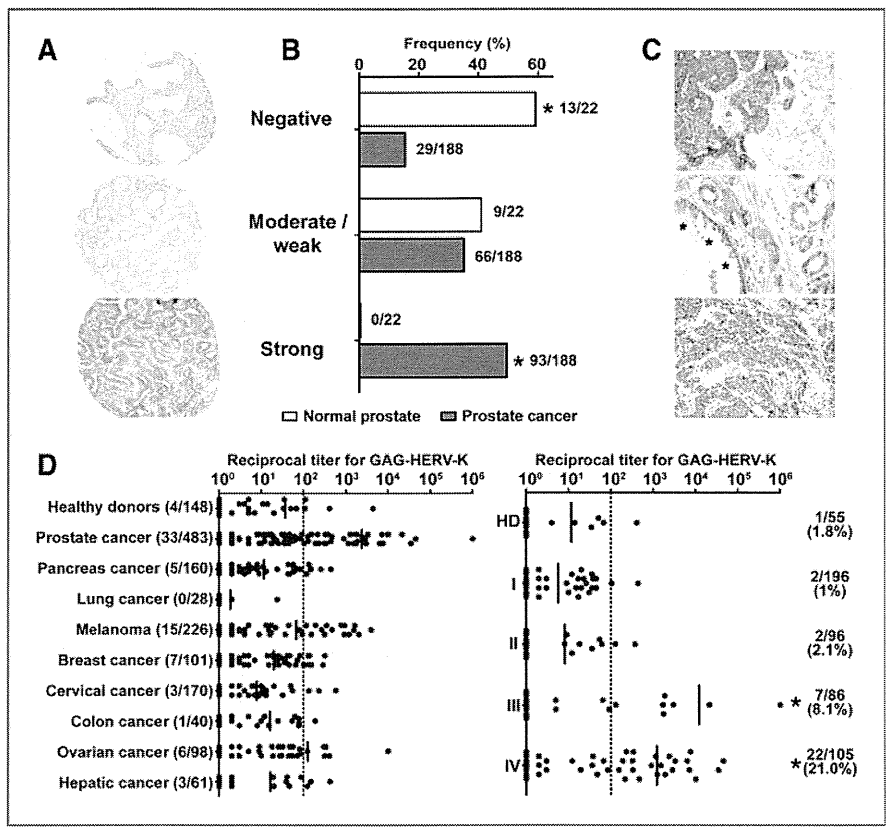

Figure 4. Tissue expression of GAG-HERV-K protein and ELISA assay to detect serum antibodies against GAG-HERV-K in patients with cancer. A, immunohistochemical analysis of GAG-HERV-K expression in paraffin sections of tissue punches of TMA with normal prostate (top) and prostate carcinoma (middle, bottom) with mAb TI-35, showing a negative staining (top), low staining (middle), and strong staining (bottom) (diaminobenzidine chromogen, brown, original magnification: 10×). B, summary of frequency of immunohistochemical staining for GAG-HERV-K in a set of prostate cancer and normal prostate TMA. C, top, immunohistochemical staining with TI-35 in whole block section of a metastatic prostate carcinoma site in lung. Middle, variable intensity of TI-35 immunostaining with more intense labeling of prostate carcinoma cells next to non-cancerous (asterisks) epithelia (original magnification: 20×). Bottom, breast carcinoma with strong homogeneous TI-35 immunostaining of invasive carcinoma cells (original magnification: 10×). D, left, sera from patients with cancer and healthy donors (HD) were tested for circulating IgG antibody reactivity against GAG-HERV-K protein by ELISA. Results are plotted as reciprocal antibody titer after confirmation of specificity using control antigens. Each dot represents a representative titer from a patient serum or healthy donor serum. Right, patients with prostate cancer were split in 4 groups according to clinical stage from I to IV, along with male healthy donors (HD). Black lines represent the mean titer of all sera for each group. Dashed lines represent the cutoff above which reactivity is considered specific (100). Percentage of positive sera represented by number of positive sera (titer higher than 1:100) per number of sera in each group. *, $P < 0.01$ by either ANOVA test (titer comparison for III or IV vs. HD or I or II) or Fisher exact test (frequency positive in IV vs. HD).

progression and the GAG-HERV-K ch22q11.23 immune response.

Antibodies to GAG-HERV-K ch22q11.23 as a biomarker for clinical staging of prostate cancer

To evaluate the correlation between antibodies to GAG-HERV-K and prostate cancer progression, sera from patients with prostate cancer were divided in 4 groups according to clinical stage (I–IV) and analyzed for the presence of antibody to GAG-HERV-K protein by ELISA. Sex-matched healthy donor sera were used as control. We found that 21.0% (22 of 105) of patients with advanced prostate cancer with stage IV disease developed antibodies to GAG-HERV-K with titers over 100, whereas only 1.0% (2 of 196) and 2.1% (2 of 96) of patients with early prostate cancer with stage I and II disease developed this response, respectively (Fig. 4D, right). Patients with stage III disease showed approximately 8.1% (7 of 86) of sera positive to GAG-HERV-K protein. Only 1 of 55 (1.8%) age-matched male healthy donors had antibodies to GAG-HERV-K protein higher than the cutoff (Fig. 4D, right). Together, presence of serum antibodies to GAG-HERV-K was significantly higher in patients with advanced cancer compared with early-stage patients or healthy donors [$P < 0.01$ with exact Fisher test (stage IV vs. HD), as well as with ANOVA comparison of all stages taking titers into account]. We also divided patients according to risk groups, based on Gleason score and eventual metastases (Table 1), and observed a similar trend, in which the highest frequency of antibodies to GAG-HERV-K was observed in patients with the highest risk group (Gleason

Published OnlineFirst September 30, 2013; DOI: 10.1158/1078-0432.CCR-12-3580

score ≥7 and eventual metastases) when compared with sex-matched healthy donor sera and other risk groups (Supplementary Fig. S5A). Independently of metastases, when considering Gleason score alone, serum antibodies to GAG-HERV-K were also significantly more frequent in patients with a Gleason score ≥ 8, compared with patients with score ≤ 6, even though not all presenting metastatic cases could be graded (Supplementary Fig. S5B). These results show a clear correlation between eventual prostate cancer progression and detection of antibody to GAG-HERV-K in patients with prostate cancer at time of biopsy, highlighting the importance of HERV-K ch22q11.23 as a predictive biomarker of tumor burden and progression.

Antibodies to self-antigens in prostate cancer GAG-HERV-K Ab$^+$ group

As the previous results unveiled, only a subset of patients with advanced prostate cancer develops antibodies to GAG-HERV-K protein. To evaluate whether patients seropositive for GAG-HERV-K may have overall differences in their immunologic response to prostate cancer and/or against self-antigens compared with GAG-HERV-K antibody-negative patients, sera from 28 patients with prostate cancer with stage IV disease were divided in 2 groups according to presence of antibodies to GAG-HERV-K (HERV-K$^+$: n = 28 and HERV-K$^-$: n = 14) and analyzed for serum antibody profiling using custom-made protein microarrays (Protoarrays with GAG-HERV-K and other cancer antigens added). Sera from sex- and age-matched healthy donors were used as control (n = 14). By applying statistical analyses described previously (32), we were able to identify several antigens that were co-recognized by the HERV-K$^+$ group (Supplementary Table S1). By comparing results from ELISA and seromic profiling, we could validate the microarray results: 89% of samples expected positive for GAG-HERV-K by ELISA were also reactive to GAG-HERV-K on the microarray, missing only 3 patients with low titer samples (data not shown). NY-ESO-1 (18%; 5 of 28) and CCNB1 (18%; 5 of 28) were the most frequently recognized antigens by the HERV-K$^+$ group. NY-ESO-1 expression has been associated with advanced prostate cancer (38) and CCNB1 autoantibody has been described in several other cancer types (39, 40). On the other hand, patients in the HERV-K$^-$ group preferentially recognized antigens such as TMP4 (29%; 4 of 14), TLE4 (29%; 4 of 14), and ARID3A (29%; 4 of 14), which have been linked to leukemias or lymphomas (41–43). Moreover, ARID3A is regulated by p53 and is a proposed target for cancer immunotherapy (43). This analysis shows heterogeneity of the immune response to cancer antigens among patients with prostate cancer with stage IV disease. Understanding the correlation between prostate cancer progression and antigen-specific immune responses could unveil individual etiologies in patients with prostate cancer.

Associations with overall survival and biochemical recurrence

To determine whether the anti-HERV-K immune response in prostate cancer can predict progression of disease, patients were divided in 2 groups based on the presence of anti-GAG-HERV-K antibodies and analyzed for overall survival using the Kaplan–Meier method. This analysis could only be conducted on a subset of 284 patients undergoing radical prostatectomy with available clinical follow-up data. This cohort unfortunately included only patients with localized disease at the time of surgery when sera were obtained and therefore did not include any clinical stage IV patients. Patients were stratified and censored according to serological reactivity against GAG-HERV-K at the time of surgery. Patients were retrospectively categorized and assessed for subsequent biochemical recurrence and metastases (risk group 1: n = 102; risk group 2: n = 96; risk group 3: n = 86; see clinical characteristics in Table 1). Although not reaching significance by log-rank test [P = 0.053; HR = 1.98 (1.23---11.85)], there was a correlation with mortality in the GAG-HERV-K antibody-positive group when compared with the GAG-HERV-K antibody–negative group using the Gehan–Breslow–Wilcoxon test (P = 0.006; Fig. 5A). We also assessed whether there was a correlation between presence of anti-GAG-HERV-K antibodies and biochemical recurrence of the disease (BCR), based on PSA levels. BCR is associated with a

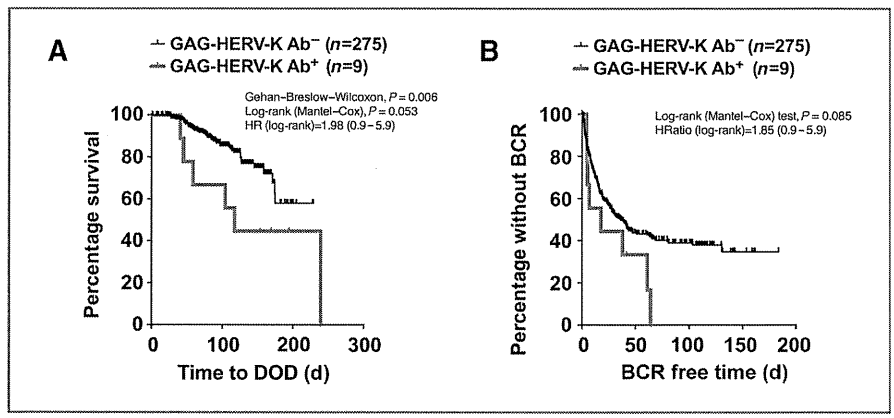

Figure 5. Overall survival curve and BCR free curve of GAG-HERV-K seropositive patients with prostate cancer. A and B, patients with prostate cancer were divided in 2 groups: GAG-HERV-K Ab$^+$ (antibodies to GAG-HERV-K with titers higher than 1:100) and GAG-HERV-K Ab$^-$ (titers lower than 1:100) and survival curve was plotted with the Kaplan-=Meier method based on time to death of disease (DOD; A) or based on time to biochemical recurrence (BCR) of PSA (B). Statistics used are indicated. d, days.

Published OnlineFirst September 30, 2013; DOI: 10.1158/1078-0432.CCR-12-3580

high likelihood of metastatic progression or prostate cancer–specific mortality (44). Although not statistically significant, there was a trend for greater BCR in prostate cancer patients seropositive for GAG-HERV-K ($P = 0.085$, by log-rank) compared with the seronegative group (Fig. 5B). The association of GAG-HERV-K serum antibodies with worse survival or greater BCR was explained by the exclusive presence of antibody to GAG-HERV-K in the high-risk groups and none in the lower risk group. However, there was no significant correlation between seropositivity for GAG-HERV-K and metastasis-free survival. Together with the observed higher frequency of antibody responses to GAG-HERV-K in stage IV patients, these results suggest that the presence of antibodies to GAG-HERV-K may be associated with a worse prognosis for patients with prostate cancer and may be indicative of relapse of disease.

Discussion

In the last decade, several studies have shown correlations between HERV expression and human disease such as multiple sclerosis (15, 19, 45). Moreover, immune responses to endogenous retrovirus derived proteins have also been correlated to cancer (20, 21, 23, 46), but no clear clinical significance has yet been suggested. Here, we identify an HERV-K GAG protein, located on chromosome 22q11.23, highly expressed in prostate cancer and capable of generating a specific immune response in advanced stages of prostate cancer.

The HERV-K located on ch22q11.23 is a complete retrovirus element, with *GAG*, *POL*, and *ENV* genes, flanked by an LTR sequence. The *POL* and *ENV* genes have mutations and/or deletions that prevent the proteins from being translated. In contrast, the *GAG* gene has a complete ORF that translates to a protein of 715 amino acids. Restricted expression of GAG-HERV-K ch22q11.23 in prostate cancer tissue suggests this molecule as a suitable biomarker and target for prostate cancer. The expression analysis of the surrounding genes located on chromosome 22q11.23 showed that expression of *GAG-HERV-K* is not due to unspecific region activation in prostate cancer.

The transcriptional program of androgenic signaling in the prostate consists of thousands of gene targets whose products play a role in almost all cellular functions, including cellular proliferation, survival, lipid metabolism, and differentiation (47). Here, we showed that androgen hormone DHT was able to upregulate the expression of GAG-HERV-K in VCaP cell line. Although VCaP and LNCaP are AR-positive, we were only able to stimulate GAG-HERV-K expression in VCaP cells. One possible explanation is that VCaP cells have higher levels of AR than LNCaP cells, thus rendering the cells more sensitive to DHT. It is well known that prostate cancer cells can overexpress AR and be more sensitive to androgen hormones (48, 49), which could contribute to the increased expression of GAG-HERV-K observed in prostate cancer samples. Using PROMO, a virtual laboratory for the identification of putative transcription factor–binding sites in DNA sequences, we found 2 potential AR-binding site at positions 328 to 336 and 496 to 504 of the promoter of *GAG-HERV-K* (from its 990 nucleotide upstream sequence). We observed that the DNA methylation status of the HERV-K promoter region (LTR) contributes to *GAG-HERV-K* expression in cancer cell lines. In accordance with our findings, HERV-K from chromosome 22q11.23 was recently observed to be highly expressed in prostate cancer samples and the expression was dependent on LTR region demethylation (37). Nevertheless, methylation is just one of several mechanisms that impact chromatin structure and gene expression, and it is possible that some of the heterogeneity in *GAG-HERV-K* expression observed among cancer cell lines may relate to differences in other possible pathways (acetylation, etc.) used to regulate the chromatin structure in the promoter region of *GAG-HERV-K*. Such mechanisms might reflect different subtypes or stages of prostate cancer, and some of the differences in the induction of GAG-HERV-K observed by androgen treatment may be related to transformation in cell cultures.

Recently, an interesting translocation event in prostate cancer has brought attention to the promoter region of HERV-K. The *HERV-K ch22q11.23* 5′LTR region was shown to be fused with *ETV1* leading to an overexpression of the gene in patients with prostate cancer (17). Importantly, *ETV1* overexpression in prostate cells confers invasiveness. It is not clear whether the HERV-K 5′LTR region alone is sufficient to activate *EVT1* expression in these patients. However, our results suggest that the 5′LTR promoter region from HERV-K not only is active but can also increase expression in response to androgen hormone stimulation, in accordance with previous findings (37). Taken together, these findings highlight the importance of HERV-K activity in prostate cancer.

Specific immune response to endogenous retrovirus components is well described in the field (20, 21, 23, 46), but no clear correlation to cancer progression has yet been determined. In this work, we showed that patients with advanced prostate cancer have a higher incidence of humoral immune response to GAG-HERV-K protein, suggesting an increase in gene expression due to prostate cancer progression. Unfortunately, none of the cohorts that we had access to allowed us to ask whether there is a direct correlation between antigen expression and antibody response, as we could only collect patient serum or tumor, but not both simultaneously. It is known that during prostate cancer progression, hypomethylation of DNA occurs and this event culminates in the expression of endogenous retrovirus (50, 51). Such increase in gene expression could lead to a specific immune response in patients with prostate cancer with the progression of the disease. Indeed, our result suggests that progression of prostate cancer is directly correlated to increase of humoral response to GAG-HERV-K protein.

Clinical staging of prostate cancer is important in assessing the risk of the disease and therefore for treatment recommendations (26). Our results indicate that GAG-HERV-K could be a useful tool for diagnostic and/or clinical stage biomarker in prostate cancer. Although we could not detect significant levels of GAG-HERV-K expression in other

Published OnlineFirst September 30, 2013; DOI: 10.1158/1078-0432.CCR-12-3580

cancer type, we detected serum antibody to GAG-HERV-K in a number of patients with melanoma, breast, and ovarian cancer, albeit at lower titers compared with patients with prostate cancer. Expression of GAG-HERV-K was also seen by IHC in other tumor tissues than prostate, although it may have been missed by qPCR in the small panel of cancer samples we used to assess it. Although the presence of autoantibodies to endogenous retrovirus proteins has been correlated to a worse clinical prognostic in patients with melanoma (23), we could not determine any correlation between presence of antibody to GAG-HERV-K ch22q11.23 and clinical staging in melanoma or ovarian cancer (data not shown).

Protein microarray profiling analysis of serum from patients with advanced prostate cancer suggests that the presence of antibodies to GAG-HERV-K is linked to other antigen-specific immune responses. An increased humoral immune response to cancer testis antigen NY-ESO-1 was observed in the GAG-HERV-K Ab^+ group. The presence of antibodies to cancer testis (CT) antigens has been associated with a worse prognosis in several cancer types including prostate cancer (32, 38, 52). The evidence of a co-immune response to GAG-HERV-K and NY-ESO-1 in a subset of patients with advanced prostate cancer suggests a potential biologic association between these 2 genes during prostate cancer progression and deserves to be further investigated.

We believe that specific expression of GAG-HERV-K in prostate cancer occurs by the combination of epigenetic modification, such as demethylation, and androgen hormone stimulation. Whether the expression of GAG-HERV-K is a causal event or a biologic consequence of prostate cancer progression still needs to be addressed. Nevertheless, we show here a clear correlation between the tissue-specific GAG-HERV-K protein expression and development of a specific immune response with progression of prostate cancer. Moreover, patients who developed antibodies to GAG-HERV-K also had a lower survival rate and appeared to have higher incidence of disease relapse (BCR). BCR is correlated with an increased mortality and metastatic events in prostate cancer and the early detection of disease relapse is crucial for an efficient treatment (44).

In conclusion, we characterized a GAG protein from a human endogenous retrovirus (HERV-K) located on chromosome 22q11.23 highly expressed in prostate cancer. The expression of GAG-HERV-K is capable of inducing humoral immune response in patients with prostate cancer. This immune response was correlated to advanced stages of the disease possibly due to increase in androgen hormone stimulation and demethylation events triggered by prostate cancer progression. The presence of serum antibodies to GAG-HERV-K was also indicative of worse prognosis and higher BCR among patient with advanced prostate cancer. Because of its restricted expression and its ability to elicit a strong humoral response, GAG-HERV-K antigen might be used as an important biomarker for prognostic purposes as well as serving as a target for immunotherapy of advanced prostate cancer. Future directions should address whether GAG-HERV-K serum antibodies change with treatment such as androgen deprivation, or during natural evolution in patients with hormone-refractory disease.

Disclosure of Potential Conflicts of Interest

H.I. Scher is a consultant/advisory board member of Veridex. No potential conflicts of interest were disclosed by the other authors.

Authors' Contributions

Conception and design: B.S. Reis, A.A. Jungbluth, Y. Obata, H.I. Scher, G. Ritter, L.J. Old, S. Gnjatic

Development of methodology: B.S. Reis, E. Nakayama, Y. Obata, H.I. Scher, J. Melamed, S. Gnjatic

Acquisition of data (provided animals, acquired and managed patients, provided facilities, etc.): B.S. Reis, A.A. Jungbluth, M. Holz, T. Ishida, B.S. Carver, H.I. Scher, P.T. Scardino, S.F. Slovin, J. Melamed, E. Jäger, G. Ritter

Analysis and interpretation of data (e.g., statistical analysis, biostatistics, computational analysis): B.S. Reis, A.A. Jungbluth, E. Ritter, B.S. Carver, H.I. Scher, S.F. Slovin, V.E. Reuter, C. Savage, J.P. Allison, G. Ritter, S. Gnjatic

Writing, review, and/or revision of the manuscript: B.S. Reis, A.A. Jungbluth, Y. Obata, B.S. Carver, H.I. Scher, P.T. Scardino, S.F. Slovin, S.K. Subudhi, V.E. Reuter, E. Jäger, G. Ritter, S. Gnjatic

Administrative, technical, or material support (i.e., reporting or organizing data, constructing databases): D. Frosina, E. Ritter, T. Ishida, H.I. Scher, S.F. Slovin, V.E. Reuter, J. Melamed, S. Gnjatic

Study supervision: H.I. Scher, G. Ritter, S. Gnjatic

Acknowledgments

The authors thank Dr. Jianda Yuan for access to serum samples at MSKCC and Angel Cronin for help with the analysis of the clinical data from MSKCC.

Grant Support

This study was funded by the Ludwig Institute for Cancer Research with additional grant support from the Cancer Research Institute. B.S. Reis was partially funded by a grant from the Brazilian agency CNPq.

The costs of publication of this article were defrayed in part by the payment of page charges. This article must therefore be hereby marked *advertisement* in accordance with 18 U.S.C. Section 1734 solely to indicate this fact.

Received November 20, 2012; revised August 26, 2013; accepted September 9, 2013; published OnlineFirst September 30, 2013.

References

1. Mayer J, Meese E. Human endogenous retroviruses in the primate lineage and their influence on host genomes. Cytogenet Genome Res 2005;110:448–56.
2. Tonjes RR, Lower R, Boller K, Denner J, Hasenmaier B, Kirsch H, et al. HERV-K: the biologically most active human endogenous retrovirus family. J Acquir Immune Defic Syndr Hum Retrovirol 1996;13 Suppl 1: S261–7.
3. Lavie L, Kitova M, Maldener E, Meese E, Mayer J. CpG methylation directly regulates transcriptional activity of the human endogenous retrovirus family HERV-K(HML-2). J Virol 2005;79: 876–83.
4. Schulz WA, Steinhoff C, Florl AR. Methylation of endogenous human retroelements in health and disease. Curr Top Microbiol Immunol 2006;310:211–50.
5. Szpakowski S, Sun X, Lage JM, Dyer A, Rubinstein J, Kowalski D, et al. Loss of epigenetic silencing in tumors preferentially affects primate-specific retroelements. Gene 2009;448:151–67.
6. Stengel S, Fiebig U, Kurth R, Denner J. Regulation of human endogenous retrovirus-K expression in melanomas by CpG methylation. Genes Chromosomes Cancer 2010;49:401–11.
7. Stoye JP, Moroni C, Coffin JM. Virological events leading to spontaneous AKR thymomas. J Virol 1991;65:1273–85.

Published OnlineFirst September 30, 2013; DOI: 10.1158/1078-0432.CCR-12-3580

8. Coffin JM, Stoye JP, Frankel WN. Genetics of endogenous murine leukemia viruses. Ann N Y Acad Sci 1989;567:39–49.
9. Obata Y, Stockert E, DeLeo AB, O'Donnell PV, Snyder HW Jr, Old LJ. A cell surface antigen of the mouse related to xenotropic MuLv defined by naturally occurring antibody and monoclonal antibody. Relation to Gix G(rada1), G(aksl2) systems of MuLV-related antigens. J Exp Med 1981;154:659–75.
10. Stockert E, O'Donnell PV, Obata Y, Old LJ. Inhibition of AKR leukemogenesis by SMX-1, a dualtropic murine leukemia virus. Proc Natl Acad Sci U S A 1980;77:3720–4.
11. Stockert E, DeLeo AB, O'Donnell PV, Obata Y, Old LJ. G(AKSL2): a new cell surface antigen of the mouse related to the dualtropic mink cell focus-inducing class of murine leukemia virus detected by naturally occurring antibody. J Exp Med 1979;149:200–15.
12. DeLeo AB, Shiku H, Takahashi T, John M, Old LJ. Cell surface antigens of chemically induced sarcomas of the mouse. I. Murine leukemia virus-related antigens and alloantigens on cultured fibroblasts and sarcoma cells: description of a unique antigen on BALB/c Meth A sarcoma. J Exp Med 1977;146:720–34.
13. Chen YT. Cancer vaccine: identification of human tumor antigens by SEREX. Cancer J 2000;6 Suppl 3:S208–17.
14. Jager D. Potential target antigens for immunotherapy identified by serological expression cloning (SEREX). Methods Mol Biol 2007;360: 319–26.
15. Ishida T, Obata Y, Ohara N, Matsushita H, Sato S, Uenaka A, et al. Identification of the HERV-K gag antigen in prostate cancer by SEREX using autologous patient serum and its immunogenicity. Cancer Immun 2008;8:15.
16. Hermans KG, van der Korput HA, van Marion R, van de Wijngaart DJ, Ziel-van der Made A, Dits NF, et al. Truncated ETV1, fused to novel tissue-specific genes, and full-length ETV1 in prostate cancer. Cancer Res 2008;68:7541–9.
17. Tomlins SA, Laxman B, Dhanasekaran SM, Helgeson BE, Cao X, Morris DS, et al. Distinct classes of chromosomal rearrangements create oncogenic ETS gene fusions in prostate cancer. Nature 2007; 448:595–9.
18. Lee YN, Bieniasz PD. Reconstitution of an infectious human endogenous retrovirus. PLoS Pathog 2007;3:e10.
19. Herbst H, Sauter M, Mueller-Lantzsch N. Expression of human endogenous retrovirus K elements in germ cell and trophoblastic tumors. Am J Pathol 1996;149:1727–35.
20. Boller K, Janssen O, Schuldes H, Tonjes RR, Kurth R. Characterization of the antibody response specific for the human endogenous retrovirus HTDV/HERV-K. J Virol 1997;71:4581–8.
21. Rakoff-Nahoum S, Kuebler PJ, Heymann JJ, E Sheehy M, Ortiz GM, S Ogg G, et al. Detection of T lymphocytes specific for human endogenous retrovirus K (HERV-K) in patients with seminoma. AIDS Res Hum Retroviruses 2006;22:52–6.
22. Schiavetti F, Thonnard J, Colau D, Boon T, Coulie PG. A human endogenous retroviral sequence encoding an antigen recognized on melanoma by cytolytic T lymphocytes. Cancer Res 2002;62:5510–6.
23. Hahn S, Ugurel S, Hanschmann KM, Strobel H, Tondera C, Schadendorf D, et al. Serological response to human endogenous retrovirus K in melanoma patients correlates with survival probability. AIDS Res Hum Retroviruses 2008;24:717–23.
24. Wang-Johanning F, Radvanyi L, Rycaj K, Plummer JB, Yan P, Sastry KJ, et al. Human endogenous retrovirus K triggers an antigen-specific immune response in breast cancer patients. Cancer Res 2008;68: 5869–77.
25. Jemal A, Siegel R, Ward E, Murray T, Xu J, Smigal C, et al. Cancer statistics, 2006. CA Cancer J Clin 2006;56:106–30.
26. Borley N, Feneley MR. Prostate cancer: diagnosis and staging. Asian J Androl 2009;11:74–80.
27. Ilic D, Green S. Prostate specific antigen for detecting early prostate cancer. BMJ 2009;339:b3572.
28. Stark JR, Mucci L, Rothman KJ, Adami HO. Screening for prostate cancer remains controversial. BMJ 2009;339:b3601.
29. Bensalah K, Lotan Y, Karam JA, Shariat SF. New circulating biomarkers for prostate cancer. Prostate Cancer Prostatic Dis 2008;11: 112–20.
30. Steuber T, O'Brien MF, Lilja H. Serum markers for prostate cancer: a rational approach to the literature. Eur Urol 2008;54:31–40.
31. Lee MS, Igawa T, Chen SJ, Van Bemmel D, Lin JS, Lin FF, et al. p66Shc protein is upregulated by steroid hormones in hormone-sensitive cancer cells and in primary prostate carcinomas. Int J Cancer 2004; 108:672–8.
32. Gnjatic S, Old LJ, Chen YT. Autoantibodies against cancer antigens. Methods Mol Biol 2009;520:11–9.
33. Cheeseman IM, Desai A. A combined approach for the localization and tandem affinity purification of protein complexes from metazoans. Sci STKE 2005;2005:pl1.
34. Gnjatic S, Ritter E, Buchler MW, Giese NA, Brors B, Frei C, et al. Seromic profiling of ovarian and pancreatic cancer. Proc Natl Acad Sci U S A 2010;107:5088–93.
35. Cremer T, Kreth G, Koester H, Fink RH, Heintzmann R, Cremer M, et al. Chromosome territories, interchromatin domain compartment, and nuclear matrix: an integrated view of the functional nuclear architecture. Crit Rev Eukaryot Gene Expr 2000;10: 179–212.
36. Gimenez J, Montgiraud C, Pichon JP, Bonnaud B, Arsac M, Ruel K, et al. Custom human endogenous retroviruses dedicated microarray identifies self-induced HERV-W family elements reactivated in testicular cancer upon methylation control. Nucleic Acids Res 2010;38: 2229–46.
37. Goering W, Ribarska T, Schulz WA. Selective changes of retroelement expression in human prostate cancer. Carcinogenesis 2011;32:1484–92.
38. Nakada T, Noguchi Y, Satoh S, Ono T, Saika T, Kurashige T, et al. NY-ESO-1 mRNA expression and immunogenicity in advanced prostate cancer. Cancer Immun 2003;3:10.
39. Hoffmann TK, Trellakis S, Okulicz K, Schuler P, Greve J, Arnolds J, et al. Cyclin B1 expression and p53 status in squamous cell carcinomas of the head and neck. Anticancer Res 2011;31:3151–7.
40. Covini G, Chan EK, Nishioka M, Morshed SA, Reed SI, Tan EM. Immune response to cyclin B1 in hepatocellular carcinoma. Hepatology 1997;25:75–80.
41. Cools J, Wlodarska I, Somers R, Mentens N, Pedeutour F, Maes B, et al. Identification of novel fusion partners of ALK, the anaplastic lymphoma kinase, in anaplastic large-cell lymphoma and inflammatory myofibroblastic tumor. Genes Chromosomes Cancer 2002;34:354–62.
42. Greif PA, Eck SH, Konstandin NP, Benet-Pages A, Ksienzyk B, Dufour A, et al. Identification of recurring tumor-specific somatic mutations in acute myeloid leukemia by transcriptome sequencing. Leukemia 2011;25:821–7.
43. Liu G, Huang YJ, Xiao R, Wang D, Acton TB, Montelione GT. Solution NMR structure of the ARID domain of human AT-rich interactive domain-containing protein 3A: a human cancer protein interaction network target. Proteins 2010;78:2170–5.
44. Stephenson AJ, Kattan MW, Eastham JA, Dotan ZA, Bianco FJ Jr, Lilja H, et al. Defining biochemical recurrence of prostate cancer after radical prostatectomy: a proposal for a standardized definition. J Clin Oncol 2006;24:3973–8.
45. Sauter M, Schommer S, Kremmer E, Remberger K, Dolken G, Lemm I, et al. Human endogenous retrovirus K10: expression of Gag protein and detection of antibodies in patients with seminomas. J Virol 1995;69:414–21.
46. Wang-Johanning F, Rycaj K, Plummer JB, Li M, Yin B, Frerich K, et al. Immunotherapeutic potential of anti-human endogenous retrovirus-k envelope protein antibodies in targeting breast tumors. J Natl Cancer Inst 2012;104:189–210.
47. Lamont KR, Tindall DJ. Androgen regulation of gene expression. Adv Cancer Res 2010;107:137–62.
48. Linja MJ, Savinainen KJ, Saramaki OR, Tammela TL, Vessella RL, Visakorpi T. Amplification and overexpression of androgen receptor gene in hormone-refractory prostate cancer. Cancer Res 2001;61: 3550–5.
49. Ford OH 3rd, Gregory CW, Kim D, Smitherman AB, Mohler JL. Androgen receptor gene amplification and protein expression in recurrent prostate cancer. J Urol 2003;170:1817–21.

Published OnlineFirst September 30, 2013; DOI: 10.1158/1078-0432.CCR-12-3580

50. Florl AR, Steinhoff C, Muller M, Seifert HH, Hader C, Engers R, et al. Coordinate hypermethylation at specific genes in prostate carcinoma precedes LINE-1 hypomethylation. Br J Cancer 2004;91:985–94.
51. Yegnasubramanian S, Haffner MC, Zhang Y, Gurel B, Cornish TC, Wu Z, et al. DNA hypomethylation arises later in prostate cancer progression than CpG island hypermethylation and contributes to metastatic tumor heterogeneity. Cancer Res 2008;68:8954–67.
52. Suyama T, Shiraishi T, Zeng Y, Yu W, Parekh N, Vessella RL, et al. Expression of cancer/testis antigens in prostate cancer is associated with disease progression. Prostate 2010;70:1778–87.

T-cell receptor repertoires of tumor-infiltrating lymphocytes after hyperthermia using functionalized magnetite nanoparticles

Aim: Accumulating evidence has indicated that hyperthermia using magnetite nanoparticles induces anti-tumor immunity. This study investigated the diversity of T-cell receptors (TCRs) in tumor-infiltrating lymphocytes after hyperthermia using magnetite nanoparticles. **Materials & methods:** Functionalized magnetite nanoparticles, *N*-propionyl-4-*S*-cysteaminylphenol (NPrCAP)/magnetite, were synthesized by conjugating the melanogenesis substrate NPrCAP with magnetite nanoparticles. NPrCAP/magnetite nanoparticles were injected into B16 melanomas in C57BL/6 mice, which were subjected to an alternating magnetic field for hyperthermia treatment. **Results:** Enlargement of the tumor-draining lymph nodes was observed after hyperthermia. The TCR repertoire was restricted in tumor-infiltrating lymphocytes, and expansion of Vβ11$^+$ T cells was preferentially found. DNA sequences of the third complementarity-determining regions revealed the presence of clonally expanded T cells. **Conclusion:** These results indicate that the T-cell response in B16 melanomas after hyperthermia is dominated by T cells directed toward a limited number of epitopes and that epitope-specific T cells frequently use a restricted TCR repertoire.

Original submitted 14 May 2012; Revised submitted 30 July 2012

KEYWORDS: hyperthermia magnetite nanoparticle melanoma T-cell receptor tumor-infiltrating lymphocyte

Akira Ito*, Masaki Yamaguchi, Noriaki Okamoto, Yuji Sanematsu, Yoshinori Kawabe, Kazumasa Wakamatsu, Shosuke Ito, Hiroyuki Honda, Takeshi Kobayashi, Eiichi Nakayama, Yasuaki Tamura, Masae Okura, Toshiharu Yamashita, Kowichi Jimbow & Masamichi Kamihira

*Author for correspondence: Department of Chemical Engineering, Faculty of Engineering, Kyushu University, 744 Motooka, Nishi-ku, Fukuoka 819-0395, Japan
Tel.: +81 92 802 2753
Fax: +81 92 802 2798
akira@chem-eng.kyushu-u.ac.jp
For a full list of affiliations please see the back page

Hyperthermia is a promising approach to treat a wide variety of tumors in patients [1,2]. A major technical problem with currently available clinical hyperthermia systems, including whole-body hyperthermia [3] and local hyperthermia by radiofrequency [4], is the difficulty of heating the tumor region to the intended temperature without damaging normal tissue. Increasing temperatures above 42.5°C can kill greater numbers of tumor cells, but normal tissues are also damaged by these conventional hyperthermia systems. Therefore, the development of a tumor-targeted hyperthermia system is required. Current developments in nanotechnology have made it possible to use a nanometric heat mediator that can generate heat under an external alternating magnetic field (AMF) [5]. Magnetite (Fe_3O_4) nanoparticle-mediated hyperthermia has been a largely experimental modality that has the potential to overcome the shortcomings of conventional hyperthermia systems [6,7]. The technique involves targeting nanoparticles to tumor tissue, and then applying an AMF to induce heat generation by hysteresis loss or relaxation loss [7,8]. In recent years, remarkable advances have been seen in magnetite nanoparticle-mediated hyperthermia for both tumor-targeted magnetite nanoparticles [9,10] and AMF generators [11,12], and some of these techniques have entered clinical trials [13].

By specifically delivering the magnetite nanoparticles to the tumor site, tumor-targeted hyperthermia can be created [14–16]. Melanogenesis uniquely occurs in melanocytic cells. Thus, tyrosine analogs that are tyrosinase substrates are good candidates for melanoma-specific targeting. The melanogenesis substrate, *N*-propionyl-4-*S*-cysteaminylphenol (NPrCAP), is selectively incorporated into melanoma cells [17]. Based upon the unique biological properties of NPrCAP, the authors have established a novel nanomedicine for melanoma by conjugating NPrCAP to the surface of magnetite nanoparticles to produce NPrCAP/magnetite (NPrCAP/M), which is selectively incorporated into melanoma cells and generates heat upon exposure to AMF [18]. When mice bearing B16F1 melanoma were intraperitoneally injected with NPrCAP/M, the nanoparticles were delivered to the melanoma in the subcutis through the bloodstream [18]. However, a large part of NPrCAP/M was captured in reticuloendothelial cell systems, such as the liver and spleen, in the mice. Therefore, clinical trials using the present nanoparticles may be limited to lesional therapy against melanoma. Current methods

Future Medicine part of fsg

of delivering magnetite nanoparticles in clinical hyperthermia depend on direct injection of the functionalized magnetite nanoparticles into the tumor site [13,19]. Although the procedure is practical for easily accessible tumors including melanoma, this direct injection may limit the usefulness of magnetite nanoparticle-mediated hyperthermia for systemically metastatic melanomas. On the other hand, we have shown that heat treatment also induces anti-tumor immunity by enhancement of heat-shock protein expression [20,21]. Previously, the authors showed that hyperthermia using NPrCAP/M elicited a cytotoxic T-lymphocyte (CTL) response via the release of heat shock protein–peptide complex from degraded tumor cells [22]. Thus, even local magnetic hyperthermia could induce a form of vaccination against tumor cells and may be effective not only for primary melanoma but also for distant metastases.

$CD8^+$ CTLs play a significant role in antigen-specific immune responses to tumors. In our previous study, $CD8^+$ T cells were observed within B16 melanomas after hyperthermia using NPrCAP/M [23]. Clinically, the presence of tumor-infiltrating lymphocytes (TILs) has been considered to be a favorable prognostic indicator [24]. In general, T cells isolated from tumor-draining lymph nodes (DLNs) have also been used as a source of TILs, because these lymph nodes directly drain the tumor. TIL reactivity to antigen is mediated via T-cell receptors (TCRs) comprising α and β chains. The β chain is composed of variable (V), diversity (D), joining (J) and constant regions. TCR diversity is produced by the random insertion or deletion of nucleotides at the V(D)J junctions. The V(D)J junctions code for the putative third complementarity-determining region (CDR3), which is thought to play the most important role in antigen recognition [25]. The TCR repertoire of a T-cell population is thus defined by its different V(D)J gene usage, as well as by the CDR3 characteristics. In the present study, the TCR repertoire after hyperthermia using NPrCAP/M was studied to further understand the T-cell response to melanoma after hyperthermia using NPrCAP/M and to develop more effective cancer immunotherapy based on magnetite nanoparticle-mediated hyperthermia.

Materials & methods

Preparation of NPrCAP/M

The magnetite nanoparticles (average particle size: 10 nm) were purchased from Toda Kogyo (Hiroshima, Japan). Magnetic characterizations of the magnetite at 796 kA/m (at room temperature) were 2.0 kA/m, 63.9 Am^2/kg and 2.6 Am^2/kg for coercivity, saturation flux density and remanent flux density, respectively. The preparation of NPrCAP/M is described elsewhere [18]. Briefly, magnetite nanoparticles were coated with aminosilane and conjugated with NPrCAP via maleimide crosslinkers. The resultant NPrCAP/M were suspended in H_2O to a concentration of 40 mg/ml. Average particle size of NPrCAP/M was approximately 280 nm. The specific absorption rate value was 42.6 W/g at 118 kHz and 30.6 kA/m (384 Oe). The amount of NPrCAP incorporated with magnetite nanoparticles was approximately 60 nmol/mg as determined by hydrolysis with 6 M HCl followed by HPLC analysis of the released 4-*S*-CAP.

Cell culture & establishment of tumors in mice

Mouse B16F1 melanoma cells (American Type Culture Collection, VA, USA) were cultured in DMEM (Gibco BRL, MD, USA), supplemented with 5% fetal calf serum, 0.1 mg/ml streptomycin sulfate and 100 U/ml potassium penicillin G. Cells were grown at 37°C in a humidified atmosphere of 5% CO_2 and 95% air.

All animal experiments were approved by the Ethics Committee for Animal Experiments of the Faculty of Engineering, Kyushu University (A22-180-0). To prepare tumor-bearing mice, cell suspensions containing 5×10^5 B16F1 cells in 50 µl of phosphate-buffered saline were injected subcutaneously into the right hind foot pad of C57BL/6 mice (age: 4 weeks; Japan SLC, Hamamatsu, Japan) after anesthesia by intraperitoneal injection of pentobarbital (50 mg /kg bodyweight) on day 1.

Hyperthermia using NPrCAP/M

NPrCAP/M (50 µl; net magnetite amount: 2 mg) were injected subcutaneously into the melanoma nodule on days 3, 5 and 7. An AMF was generated using a horizontal coil (inner diameter: 7 cm; length: 7 cm) with a transistor (Dai-ichi High Frequency, Tokyo, Japan). The magnetic field frequency and intensity were 118 kHz and 30.6 kA/m (386 Oe), respectively. After the administration of NPrCAP/M, anesthetized mice were placed in the inverter coil with their foot at the center and were exposed to the AMF inside the coil for 30 min on days 3, 5 and 7. Temperatures at the tumor surface and in the rectum were measured using an optical

fiber probe (Anritsu Meter, Tokyo, Japan). The therapeutic temperature was controlled at 43°C by measuring the tumor temperature and adjusting the power of the transistor inverter throughout the AMF exposure.

The tumor was resected and weighed 2 weeks after the first treatment (on day 17). For immunohistochemical examination, tumor tissues were immediately frozen in optimal cutting temperature compound (Sakura Finetechnical, Tokyo, Japan). Thin slices (4 µm) of the frozen tumor tissues were incubated at 37°C for 60 min with rat monoclonal antibody against mouse CD8a (clone: 53-6.7, BD Pharmingen, CA, USA). These sections were subsequently incubated at 37°C for 30 min with biotinylated anti-rat IgG (Dako, Glostrup, Denmark). Specimens were incubated at 37°C for 30 min with peroxidase-conjugated streptavidin (Dako). Each step was followed by washing with Tris-buffered saline. Peroxidase activity was visualized by diaminobenzidine tetrahydrochloride–nickel solution containing 0.007% hydrogen peroxide. Slides were counterstained with methyl green. For negative controls, primary antibodies were replaced with an unrelated IgG.

Isolation of CD8$^+$ TILs & flow cytometric analysis

Mice were anesthetized and lymph nodes were resected to isolate CD8$^+$ T cells 2 weeks after the first hyperthermia treatment (on day 17). For lymph node mapping, 1% Evans blue dye (Sigma-Aldrich, MO, USA) in 25 µl Hank's buffered salt solution [26] was subcutaneously injected into the hind foot pad. The blue-labeled inguinal lymph node from the tumor side of the mouse was taken as the tumor DLN, and the contralateral inguinal lymph node was considered to be a non-DLN [27]. The diameter of lymph nodes was measured using calipers, and the size was determined by applying Equation 1:

$$\text{Lymph node volume} = 0.5\,(\text{length} \times \text{width}^2) \quad (1)$$

Single-cell suspensions of lymph nodes were prepared using the gentleMACS™ Dissociator (Miltenyi Biotec, Bergisch Gladbach, Germany). The CD8$^+$ T cells were isolated from the cell suspension by collection with CD8a (Ly-2) MicroBeads® using a MACS® MS separation column according to the manufacturer's instructions (Miltenyi Biotec). Naive mice that were born at nearly the same time were used as controls. For flow cytometric analysis of CD8, the CD8$^+$ T cells were isolated from the cell suspension by negative selection using a CD8a$^+$ T-cell Isolation kit and a MACS MS separation column according to the manufacturer's instructions (Miltenyi Biotec). For single staining of CD8, the cells that were obtained from the negative selection were mixed and stained with phycoerythrin-conjugated anti-CD8 antibody (CD8a–phycoerythrin, Miltenyi Biotec). For double staining of CD8 and TCR Vβ11, the negatively selected cells were mixed and stained with both peridinin chlorophyll protein-conjugated anti-CD8 antibody (CD8–peridinin chlorophyll protein, Miltenyi Biotec) and fluorescein isothiocyanate-conjugated anti-TCR Vβ11 (clone RR3-15; BD Pharmingen). Flow cytometric analyses were performed to analyze the percentage of CD8$^+$ or CD8$^+$/TCR Vβ11$^+$ T cells using a FACSCalibur™ Flow Cytometer (BD Bioscience, NJ, USA). The number of CD8$^+$ T cells in a lymph node was calculated from the percentage of CD8$^+$ T cells in the total number of lymphocytes that were counted by the trypan blue dye exclusion method using a hemocytometer.

Reverse-transcription PCR & DNA sequencing

Expression of TCR Vβ repertoires was assessed using the SuperTCRExpress™ Mouse T Cell Receptor Vβ Repertoire Clonality Detecting Kit according to the manufacturer's protocol (BioMed Immunotech, FL, USA). This assay system comprises V(D)Jβ-specific PCR amplifications and a gel-based assay. In brief, total RNA was extracted from the CD8$^+$ T cells isolated from a lymph node or the melanoma nodule resected 2 weeks after the first hyperthermia treatment (on day 17). cDNA was synthesized from the isolated RNA, and *TCR* genes were amplified in a single step of 35 PCR cycles. A nested PCR amplified specific *TCR* genes using *TCR Vβ* gene-specific oligonucleotides after an additional 30 cycles. PCR products were resolved on a 4% high-resolution agarose gel. Clonality and diversity in the CDR3 region of the *TCR Vβ* repertoire in mouse T lymphocytes could be confirmed by examination of the *TCR Vβ* expression pattern [28]. For DNA sequencing, TCR Vβ-chain bands on a gel were cut out and purified using the MagExtractor™-PCR & Gel Clean Up Kit (Toyobo, Osaka, Japan). The amplified PCR products were cloned into the pGEM®-T vector (Promega, WI, USA). Plasmid DNA from positive colonies was sequenced using a DNA sequencer (Prism® 3130 Genetic

doi:10.2217/NNM.12.142

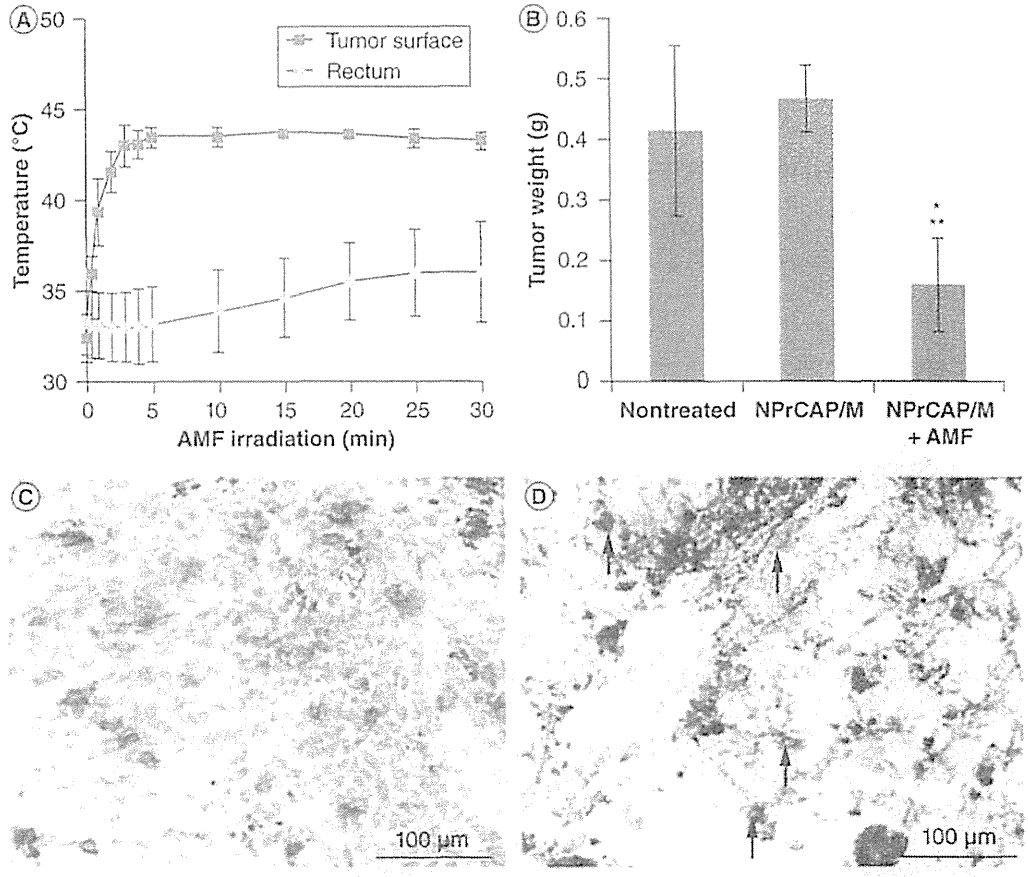

Figure 1. Hyperthermia using *N*-propionyl-4-*S*-cysteaminylphenol/magnetite.
(A) Temperatures at the tumor surface (squares) and in the rectum (circles) during AMF irradiation. NPrCAP/M were injected directly into subcutaneous B16 tumors. Data points and bars are the means and standard deviations from five mice. **(B)** Tumor weight on day 17. Untreated tumors or those injected with NPrCAP/M with or without AMF irradiation were resected, and tumor weight was measured on day 17. Data are the means and standard deviations from five mice. **(C & D)** Immunohistochemical staining for $CD8^+$ T cells **(C)** around and **(D)** within the tumor on day 17. Tumors were resected after NPrCAP/M-mediated hyperthermia. Violet-blue cells are anti-CD8 antibody-stained cells visualized by diaminobenzidine tetrahydrochloride–nickel solution containing hydrogen peroxide. Slides were counterstained with methyl green, and nuclei are light green. Arrows in **(D)** show a few representative $CD8^+$ T cells within the tumor.
*$p < 0.01$ against untreated mice.
**$p < 0.01$ against the mice treated with NPrCAP/M alone.
AMF: Alternating magnetic field; NPrCAP/M: *N*-propionyl-4-*S*-cysteaminylphenol/magnetite.

Analyzer; Applied Biosystems, CA, USA), and the sequences were compared to the GenBank database using the BLAST search engine.

Assay of amounts of IFN-γ in culture supernatants

After the hyperthermia treatment, DLNs from five mice were harvested on day 17, and lymphocytes were then restimulated *in vitro* with mitomycin C-treated B16F1 cells (1×10^7 cells) or antigen peptides (10 µg/ml) in 10 ml of RPMI-1640 supplemented with 50 µM of β-mercaptoethanol and 10% fetal calf serum for 5 days. For the restimulation, B16F1 cells were pretreated with IFN-γ (100 units/ml) for 48 h because B16 cells express MHC class I molecules at a low level, which can be enhanced by IFN-γ treatment [29]. The melanoma-associated antigen peptides used in this study were tyrosinase-related protein (TRP)-$1_{222-229}$ (amino acid sequence: TWHRYHLL; synthesized by Greiner Bio-One, Frickenhausen, Germany) [30], TRP-$2_{180-188}$ (amino acid sequence: SVYDFFVWL; Abgent, CA, USA) [31], and glycoprotein 100_{25-33} (amino acid sequence: EGSRNQDWL; AnaSpec, CA, USA) [32]. As a negative control, ovalbumin peptide ($OVA_{257-264}$; amino acid sequence: SIINFEKL peptide; Abbiotec, CA, USA) was used [33]. Purity of these peptides was >90%. After

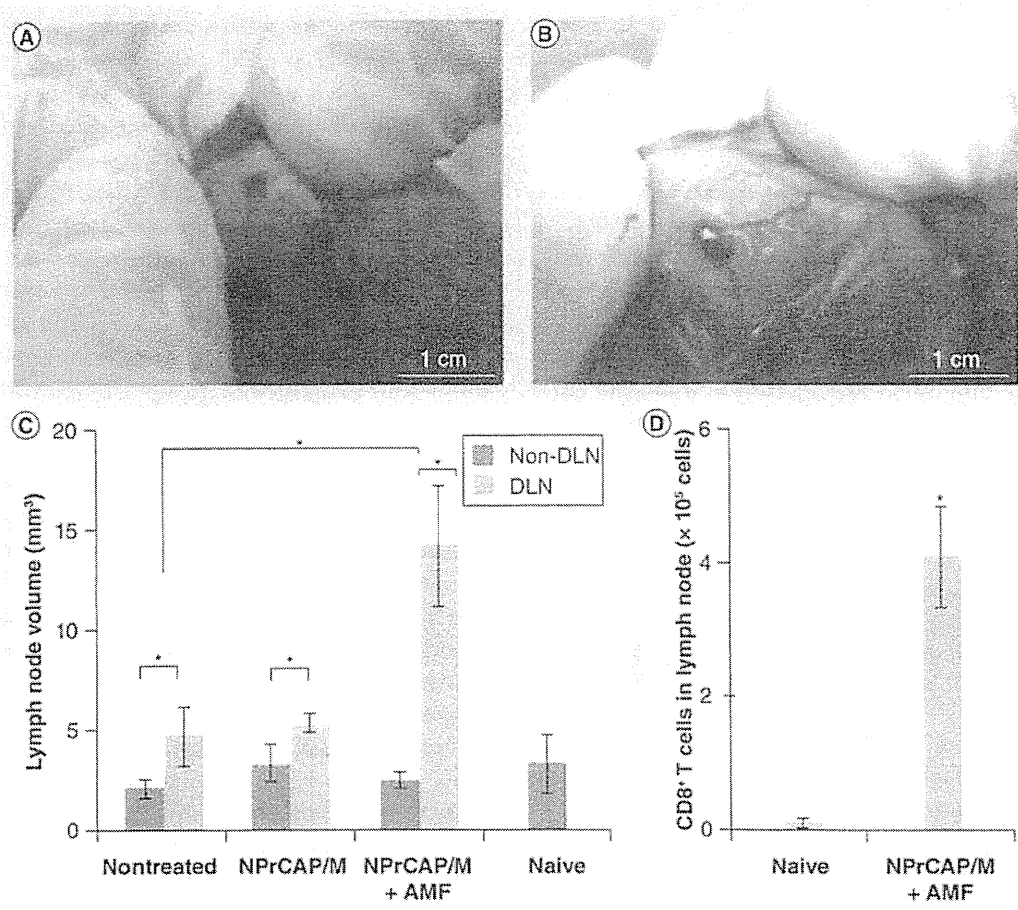

Figure 2. Analysis of lymph node after *N*-propionyl-4-*S*-cysteaminylphenol/magnetite-mediated hyperthermia. (A & B) Evans blue dye labeling of a representative inguinal **(A)** non-DLN and **(B)** DLN. On day 17, 1% Evans blue dye solution was subcutaneously injected into the hind foot pad. **(C)** Lymph node volume on day 17. Data are the means and standard deviations from five mice. **(D)** The number of $CD8^+$ T cells in a lymph node on day 17. $CD8^+$ T cells were negatively selected by magnetic cell sorting. The cells were mixed and stained with phycoerythrin-conjugated anti-CD8 antibody, and flow cytometric analyses were performed to analyze the percentage of $CD8^+$ T cells. The number of $CD8^+$ T cells in a lymph node was calculated from the percentage of $CD8^+$ T cells among the total number of lymphocytes that were counted by the trypan blue dye exclusion method using a hemocytometer. Data are the means and standard deviations from five mice.
*$p < 0.01$.
AMF: Alternating magnetic field; DLN: Draining lymph node; NPrCAP/M: *N*-propionyl-4-*S*-cysteaminylphenol/magnetite.

the restimulation, culture supernatants were collected and amounts of IFN-γ were measured by sandwich ELISA (Thermo Fisher Scientific, IL, USA) according to the manufacturer's instructions. Data were presented as picograms of IFN-γ per milliliter.

Statistical analysis

Statistical analysis was performed by the Mann–Whitney rank sum test calculated using WinSTAT statistical software (Light Stone International, Tokyo, Japan). Differences were considered to be statistically significant at $p < 0.05$.

Results & discussion

Hyperthermia by means of NPrCAP/M

For superficial melanoma, a simple heat mediator is desirable for clinical application. We previously showed the therapeutic effects of NPrCAP/M-mediated hyperthermia on B16 melanoma subcutaneously transplanted into flanks of mice [23]. In the present study, NPrCAP/M-mediated hyperthermia was performed on subcutaneous melanoma in the hind foot pad to confine the DLN to the inguinal and popliteal lymph nodes [26]. Figure 1A shows the temperature at the tumor surface and in the rectum during AMF

doi:10.2217/NNM.12.142